Published in final edited form as:
J Neurochem. 2012 September ; 122(5): 941–951. doi:10.1111/j.1471-4159.2012.07836.x.

Alterations in bioenergetic function induced by Parkinson's disease mimetic compounds: Lack of correlation with superoxide generation

Brian P. Dranka[1], **Jacek Zielonka**[1], **Anumantha G. Kanthasamy**[2], and **Balaraman Kalyanaraman**[1]

[1]Department of Biophysics and Free Radical Research Center, Medical College of Wisconsin. Milwaukee, WI

[2]Department of Biomedical Sciences, College of Veterinary Medicine, Iowa State University. Ames, IA

Abstract

In vitro and *in vivo* models of Parkinson's disease (PD) suggest that increased oxidant production leads to mitochondrial dysfunction in dopaminergic neurons and subsequent cell death. However, it remains unclear if cell death in these models is caused by inhibition of mitochondrial function or oxidant production. The objective of the present study was to determine the relationship between mitochondrial dysfunction and oxidant production in response to multiple PD neurotoxicant mimetics. MPP^+ caused a dose-dependent decrease in the basal oxygen consumption rate (OCR) in dopaminergic N27 cells, indicating a loss of mitochondrial function. In parallel, we found that MPP^+ only modestly increased oxidation of hydroethidine as a diagnostic marker of superoxide production in these cells. Similar results were found using rotenone as a mitochondrial inhibitor, or 6-hydroxydopamine as a mechanistically distinct PD neurotoxicant, but not with exposure to paraquat. Additionally, the Extracellular Acidification Rate, used as a marker of glycolysis, was stimulated to compensate for OCR inhibition after exposure to MPP^+, rotenone, or 6-hydroxydopamine, but not paraquat. Together these data indicate that MPP^+, rotenone and 6-hydroxydopamine dramatically shift bioenergetic function away from the mitochondria and towards glycolysis in N27 cells.

Keywords

mitochondria; glycolysis; reactive oxygen species; hydroethidine

Introduction

Parkinson's disease (PD) is the second most common neurodegenerative disorder in the United States, affecting an estimated 500,000 Americans, and projected to increase in prevalence (Dorsey *et al.* 2007). Current therapeutic options for patients with PD are mainly limited to symptom management (Jenner 2008). Recent research efforts have focused on mitochondrial dysfunction and overproduction of reactive oxygen and nitrogen species (ROS/RNS) as potential causal mechanisms (Yacoubian & Standaert 2009). Despite these proposals, it remains unclear whether increased ROS production in the mitochondria is the

Corresponding Author: Balaraman Kalyanaraman, Ph. D. Medical College of Wisconsin Department of Biophysics 8701 Watertown Plank Road Milwaukee, WI 53226 Phone: 414-955-4000 Fax: 414-955-6512 balarama@mcw.edu.

cause or merely a consequence of disease progression. Several current *in vitro* and *in vivo* models of PD focus on pharmacologic inhibition of mitochondrial electron transport chain (ETC) proteins (e.g., Complex I) (Cannon *et al.* 2009). Because these compounds are known inhibitors of the ETC, and the ETC is both a target and a source of ROS, the relative contribution of ROS production and ATP synthesis inhibition to eventual cell death has not been conclusively determined.

The importance of cellular oxidant status in controlling mitochondrial function is clear. Previous reports by Davey and colleagues demonstrate that elimination of the cellular antioxidant glutathione removes the threshold of complex I inhibition required to decrease ATP production (1998). Despite clear evidence that ROS is increased in PD patients, clinical trials involving the use of antioxidants for PD prevention have been unremarkable thus far (Yacoubian & Standaert 2009, Snow *et al.* 2010). One explanation for this discrepancy is that the antioxidants are applied at insufficient doses, or that the intervention occurs too late in disease progression. Alternatively, there could exist a disconnect between mitochondrial dysfunction and oxidative stress in PD progression. To address this, here we determine the correlation between inhibition of mitochondrial function and induction of superoxide production.

Over the last three decades, four main PD mimetics have been employed to study the molecular pathology of PD in cell culture – MPP^+, rotenone, 6-hydroxydopamine (6-OHDA), and paraquat (Sayre 1989, Rodriguez-Pallares *et al.* 2007). Rotenone is a known inhibitor of Complex I that blocks electron transfer to one of the 8 iron/sulfur clusters in this enzyme. MPP^+, in contrast, has no clear mechanism of inhibition, though there is evidence for diminished mitochondrial membrane potential subsequent to Nernstian uptake into the mitochondria (Sayre 1989, Scotcher *et al.* 1991). Redox cycling by MPP^+ has been proposed, but is unlikely to occur in physiological systems, owing to its high 1-electron reduction potential (Klaidman *et al.* 1993). Separate from both of these compounds, 6-OHDA is a toxic metabolite of dopamine which is a substrate for the catecholamine reuptake system, yielding specificity for dopaminergic neurons when administered *in vitro* or *in vivo* (Rodriguez-Pallares *et al.* 2007, Latchoumycandane *et al.* 2011). The mechanism of action is thought to be a combination of oxidant production secondary to metal-catalyzed 6-OHDA autooxidation, inhibition of mitochondrial Complex I, and NADPH oxidase activation in microglial cells (Gee & Davison 1989, Rodriguez-Pallares *et al.* 2007). Paraquat is an herbicide that has been associated with increased PD risk in farmers with high exposure to the compound (Tanner *et al.* 2011). Similar to the compounds discussed above, the proposed mechanism of paraquat toxicity is through the generation of ROS. In contrast to MPP^+, ROS generation by paraquat has been suggested to largely occur due to redox cycling with mitochondrial NADH dehydrogenase (E.C. 1.6.5.3) (Frank *et al.* 1987, Fukushima *et al.* 1993), and more recently ubiquinol:cytochrome c oxidoreductase (E.C. 1.10.2.2) (Castello *et al.* 2007, Drechsel & Patel 2009). This suggests that mitochondrial function may be impaired as in other models of PD (Czerniczyniec *et al.* 2011).

In sum, the common mechanisms proposed for toxicity in all of these pharmacologic models of PD center around 2 major pathways: inhibition of mitochondrial function, and increased ROS generation (either direct production from the compound, or secondary to increased inflammation)(Votyakova & Reynolds 2001). In this study, we seek to understand the relationship between mitochondrial dysfunction and superoxide production in cells treated with each of these model compounds. Because exposure to each compound results in Parkinson's disease-like symptoms in animal models (Dunnett & Lelos 2010, Ghosh *et al.* 2010, Duty & Jenner 2011), and neuronal death in cell culture models (Collier *et al.* 2003, Zhang *et al.* 2007), similar effects on mitochondrial function and ROS generation should be expected if they are working through the same mechanism. As a result, both mitochondrial

dysfunction and oxidative stress are attractive targets for clinical intervention (Schulz & Beal 1995, Beal 2003, Schapira 2012).

Methods

Cell culture and reagents

Unless otherwise stated, all chemicals used in this study were from Sigma (St. Louis, MO), and were cell-culture grade or better. The dopaminergic N27 cell line derived from rat mesencephalon was maintained in RPMI 1640 media from Invitrogen (Carlsbad, CA) essentially as described (Fukui & Moraes 2008, Jin *et al.* 2011). Culture media were supplemented with fetal bovine serum (FBS, 10%), penicillin (100 units/ml), and streptomycin (100 μg/ml), all from Invitrogen. In experiments utilizing the Seahorse Bioscience XF24, cells were changed to assay media comprised of RPMI 1640 lacking sodium bicarbonate with added sodium pyruvate (5 mM), penicillin (100 units/ml), and streptomycin (100 μg/ml), all from Invitrogen. The pH of this media was adjusted to 7.4 using dilute HCl immediately prior to use. Cells were maintained in a 37°C, humidified incubator with 5% CO_2. For extracellular flux measurements, cells were transferred to a 37°C CO_2-free incubator after changing to assay media lacking sodium bicarbonate.

HPLC analysis of hydroethidine oxidation

Oxidation of hydroethidine (HE) to 2-OH-E^+ was used as an indicator of superoxide radical anion ($O_2^{\bullet -}$) production in intact N27 cells using a previously described method (Zielonka *et al.* 2009). Non-specific oxidation to ethidium and dimeric ethidium products was also monitored as an indicator of formation of oxidants other than superoxide (Zielonka *et al.* 2012). Briefly, N27 cells were cultured in 100 mm dishes. Cells were treated as indicated for 4 h, and HE was added to a final concentration of 10 μM for the last hour of incubation. The cells were then washed twice with ice-cold Dulbecco's PBS (DPBS), and scrape-harvested into 1 ml of DPBS. The samples were centrifuged at 1000 × g for 1 min, and the supernatant discarded. The pellet was then snap frozen in liquid nitrogen. Pellets were syringe lysed using 10 strokes through a 28 ga needle in 150 μl 0.1% Triton X-100 in ice-cold PBS. HE oxidation products were then extracted using 100 μl of 0.2 M $HClO_4$ in methanol. The samples were incubated on ice for 1 h, and then centrifuged for 30 min at 20,000× g, 4°C. 100 μl of the supernatant was then transferred to a fresh tube, and the pH was adjusted with 1 M phosphate buffer, pH 2.6. This solution was centrifuged for an additional 15 min at 20,000 × g, 4°C. 150 μl of the resulting supernatant was transferred to HPLC vials for analysis. Using an Agilent 1100 HPLC system, 50 μl of each sample was resolved on a Kinetex C18 column (Phenomenex, 100 × 4.6 mm, 2.6 μm) equilibrated with 20% CH_3CN [containing 0.1% (v/v) trifluoroacetic acid (TFA)] in 0.1% TFA aqueous solution. The compounds were eluted during a linear increase in CH_3CN fraction from 20% to 60% over 5 min (using a flow rate of 1.5 ml/min). The fraction of CH_3CN was increased to 100% over the next 2 min, and maintained at that level for 1.5 min. For the quantitation of HE oxidation products, the peak area detected by the absorption detector at 370 nm (HE, HE-HE) and 290 nm (HE-E^+, E^+-E^+) as well as the fluorescence detector (excitation 358 nm, emission 440 nm for HE; excitation 490 nm, emission 567 nm for 2-OH-E^+; excitation 490 nm, emission 596 nm for E^+) were used.

Measurement of mitochondrial oxygen consumption and extracellular flux

To monitor the consumption of oxygen and extracellular acidification in intact, adherent N27 cells, a Seahorse Bioscience XF24 Extracellular Flux Analyzer was used (Seahorse Bioscience, North Billerica, MA). For these experiments, N27 cells were seeded to 4×10^4 cells/well in Seahorse Bioscience V7 polystyrene microplates. OCR was measured using mix/wait/measure times of 2 min/2 min/3 min. All data was obtained using the AKOS

algorithm in software version 1.7.0.78 (Gerencser *et al.* 2009). In some experiments, specific indices of mitochondrial function were assessed using a previously described mitochondrial function assay (Jekabsons & Nicholls 2004, Hill *et al.* 2009, Dranka *et al.* 2010). In these experiments, oligomycin (1 μg/ml), FCCP (3 μM), and antimycin A (10 μM) were injected to the indicated final concentration using the included ports on the XF24 cartridges. Further analysis of these experiments was performed using Microsoft Excel 2010 to calculate ATP-linked OCR, proton leak OCR, and the reserve capacity as described (Dranka *et al.* 2010).

ATP quantification

Intracellular ATP levels were quantified using a luminescence kit from Sigma (St. Louis, MO) essentially according to the manufacturer's instructions. Briefly, cells seeded into 96-well plates were washed twice with PBS, lysed, and samples were added to the ATP measurement reagent. Luminescence was monitored using a Beckman-Coulter DTX880 plate reader. An ATP standard curve was used to determine ATP levels in the cells.

Statistical analysis

All data were analyzed and plotted using Microsoft Excel 2010 or Origin 8.5 (OriginLab; Northampton, MA). Unless otherwise indicated, all data are the mean ± sem for an individual experiment, and representative of at least three independent experiments. Statistical significance was calculated using unpaired two-tailed t-tests. Data were considered statistically significant when $p \leq 0.05$.

Results

Superoxide production in the presence of PD mimetics is low

Superoxide production was quantified by monitoring the oxidation of HE to 2-OH-E^+ and expressed as the amount of 2-OH-E+ formed during 1 hr normalized to the amount of cellular protein in cell lysates. N27 cells were seeded in 10 cm dishes. When confluent, the cells were exposed to 150 μM MPP^+, 1 μM rotenone, 100 μM 6-OHDA, 1 mM paraquat, or 20 μM menadione. As shown in **Figure 1A**, MPP^+, rotenone, and paraquat all stimulated a slight but significant increase in the 2-OH-E^+ HPLC signal. This indicates that these compounds stimulate an approximate 2-fold increase in $O_2^{\bullet -}$ level. Surprisingly, 6-OHDA elicited no increase in this parameter. Menadione (20 μM) was used as a positive control for production of $O_2^{\bullet -}$, causing a 3.7-fold increase in 2-OH-E^+, the specific marker of HE oxidation by $O_2^{\bullet -}$. Notably, both MPP^+ and rotenone stimulated a large increase in E^+, E^+-E^+ dimer, and HE-E^+ heterodimer. These reaction products are not specific to the reaction of HE with $O_2^{\bullet -}$ (Zhao *et al.* 2003, Zielonka *et al.* 2009). Peak area from the representative HPLC traces shown in **Figure 1A** were quantified using standards for 2-OH-E^+, HE, E^+, and E^+-E^+. Levels of HE-E^+ and HE-HE dimers are expressed as the peak area per mg protein as standards for these compounds are not available. Quantification of the HPLC data is shown in **Figure 1B**.

Defining the bioenergetic profile of N27 dopaminergic neuronal cells

Before proceeding with other analyses of the effects of MPP^+ on cellular bioenergetic function, optimal conditions for using N27 cells in the Seahorse Bioscience XF24 Extracellular Flux Analyzer were established. First, an optimal seeding density for these cells was determined. As shown in **Supplemental Figure 2A**, OCR and ECAR increased linearly with respect to cell density. Based on these data, 40,000 cells/well were chosen for further experiments. Second, the role of pyruvate in OCR measurements was determined. Previous reports indicate that pyruvate supplementation is critical for accurate measurement of OCR in neuron-derived cell cultures (Jekabsons & Nicholls 2004). N27 cells were seeded

as described, and bioenergetic function was measured in assay media containing 0, 1, 5, or 10 mM sodium pyruvate. OCR was found to increase at all concentrations of pyruvate, with ≥1 mM yielding the highest stimulation of basal OCR (**Supplemental Figure 2B**) and apparent reserve capacity (**Supplemental Figure 2C**).

Inhibition of oxygen consumption by MPP^+ results in stimulation of glycolytic function in adherent N27 cells

To determine the effect of acute MPP^+ treatment on cellular bioenergetic function in intact dopaminergic N27 cells, changes in the rates of oxygen consumption as well as extracellular acidification were monitored. As shown in **Figure 2A**, injection of MPP^+ caused a dose- and time-dependent decrease in oxygen consumption. At 300 μM concentration, OCR was inhibited by 80% within 3 h. Concomitant with the inhibition of OCR, MPP^+ stimulated the Extracellular Acidification Rate (ECAR), which is used as a measure of glycolysis (Wu *et al.* 2007). Stimulation of ECAR was also found to be dose- and time-dependent with 300 μM MPP^+ causing a 30% increase over baseline (**Figure 2B**). As these measurements can be considered to be representative of whole cell bioenergetic function, plotting the response of OCR against ECAR over time shows that cells treated with 300 μM MPP^+ shift towards glycolysis (**Figure 2C**).

Rotenone inhibits mitochondrial function more rapidly than MPP^+

Rotenone exhibits known inhibitory effects on Complex I of the mitochondrial ETC, so we next tested the kinetics of rotenone's action on mitochondrial oxygen consumption. As shown in **Figure 3A and S3A**, rotenone at concentrations as low as 100 nM caused a near maximal inhibition of cellular oxygen consumption within 30 min of injection into the cell culture. Similar to the effects of MPP^+, ECAR was also stimulated in the presence of rotenone, consistent with increased glycolytic demand due to inhibition of mitochondrial ATP production (**Figure 3B, S3B**). These data thus represent a rapid switch to glycolytic metabolism as shown in **Figure 3C**, typified by decreased OCR and increased ECAR.

Paraquat stimulates oxygen consumption

Similar to experiment described above, the effect of paraquat on N27 cell bioenergetic function was assessed. As shown in **Figure 4A**, paraquat induced a small concentration-dependent stimulation of OCR over 4 h. Interestingly, the concomitantly measured ECAR shown in **Figure 4B** indicates that concentration-dependent inhibition of glycolysis is rapid and sustained for the entirety of the 4 h treatment. As expected, these data represent a fast inhibition of glycolysis and a slow stimulation of mitochondrial oxygen consumption as shown in **Figure 4C**.

Inhibition of mitochondrial oxygen consumption by PD mimetics is at the expense of ATP-Linked OCR

To determine the mechanism of inhibition of OCR shown in **Figures 2, 3, and 4**, specific indices of mitochondrial function were assessed. In the first series of experiments, N27 cells were treated with MPP^+ at a final concentration of 50, 150, or 300 μM for 4 h. The cells were then washed free of the MPP^+, and mitochondrial function was assessed as described (Dranka *et al.* 2010). Sequential additions of oligomycin (1 μg/ml), FCCP (3 μM), and antimycin A (10 μM) were used to define a mitochondrial function profile (**Supplemental Figure 4A**). This profile designates the proportion of the basal OCR that is linked to ATP production. It also allows calculation of the reserve capacity based on the measured maximal OCR in the presence of FCCP (Dranka *et al.* 2010). As shown in **Figure 5A** and **Supplemental Figure 4B**, MPP^+ inhibits basal OCR after 4 h, consistent with the data shown in **Figure 2**. This was found to be due to a loss of ATP-linked OCR (i.e., the fraction

of total oxygen consumption coupled to the production of ATP at mitochondrial Complex V). Additionally, maximal OCR as stimulated by FCCP was also found to be decreased by nearly 50% relative to control untreated cells (**Figure 5A**). Apparent reserve capacity increased after treatment with MPP^+, despite a loss in maximal OCR. This seeming paradox will be discussed further below.

N27 cells were also treated according to the same experimental design with rotenone (0.1-10 μM), 6-hydroxydopamine (6-OHDA; 50-200 μM), or paraquat (50-1000 μM). **Supplemental Figures 4C, D, and E** show the time resolved measurement of mitochondrial function as described above for cells treated with rotenone, 6-OHDA, or paraquat, respectively. As with MPP^+ treatment, both rotenone and 6-OHDA decreased basal OCR due largely to the loss of ATP-linked OCR. This occurred in a concentration-dependent manner in both rotenone and 6-OHDA treated cells. Consistent with data shown in **Figure 4**, paraquat only modestly increased the basal OCR. Interestingly, a concentration-dependent increase in the non-mitochondrial OCR was the only parameter significantly altered in response to paraquat. This will be discussed in greater detail below.

The bioenergetic shift induced by MPP^+ but not rotenone is reversible

To determine if the inhibition of OCR and stimulation of ECAR by MPP^+ is transient or permanent, cells were treated with 300 μM MPP^+ for 4 h, the media was removed and replaced with assay media, and the cells were monitored for an additional 8 h. After the cells were changed to assay media, they were incubated in a non-CO_2 incubator for 1 h prior to beginning the bioenergetics measurements as described in the methods. As shown in **Figure 6A**, OCR recovers to baseline levels after approximately 4 h. ECAR stimulation also returns to baseline concomitantly (**Figure 6B**). The normalization of ECAR at concentrations lower than 300 μM appears to happen within the 1 h media washout period as no significant stimulation of ECAR was apparent at the beginning of the assay. Interestingly, exposure to rotenone according to the same treatment scheme caused irreversible OCR inhibition as no recovery was observed within 8 h of compound washout (**Figure 6C, S3C**). Similarly, ECAR did return to control levels within 6 h following removal of rotenone at all concentrations tested (**Figure 6D**).

MPP^+ decreases mitochondrial production of ATP

Despite the stimulation of ECAR in response to MPP^+, ATP levels declined in a dose-dependent manner in the presence of MPP^+ (**Figure 7**), though this effect was modest. To determine if glycolytic ATP supports the total cellular ATP level in the presence of MPP^+, N27 cells were treated with MPP^+ (0-300 μM) in the presence of oligomycin (1μg/ml, to inhibit mitochondrial ATP synthesis) or 2-deoxy-D-glucose (2-DG, 10 mM, to inhibit glycolysis). As shown in **Figure 7**, the addition of oligomycin had no effect on ATP levels in the presence of MPP^+, but 2-DG synergized with MPP^+ to cause a further decrease in cellular ATP levels.

Discussion

One major area of interest in Parkinson's disease pathogenesis is whether increased oxidant production is a cause or merely a consequence of mitochondrial inhibition. While both of these events are well documented to occur in PD patients, the exact impact of each on the other remains unclear. The major mechanism proposed to lead to cell death in response to MPP^+ is increased ROS production following inhibition of Complex I (Johannessen *et al.* 1986, Adams *et al.* 2001). Recent techniques to examine superoxide ($O_2^{\bullet-}$) by HPLC analysis of HE reaction products allow for a more clear determination of the cause of HE oxidation (Zielonka *et al.* 2009, Zielonka & Kalyanaraman 2010). In the first series of

experiments, we examined whether $O_2^{\bullet-}$ production was increased following treatment with common PD mimetic compounds. As shown in **Figure 1**, these data reveal that 2-OH-E^+ generation is significantly lower in all treatment groups as compared to 20 μM menadione, which is used here as a positive control for $O_2^{\bullet-}$ production. Both 150 μM MPP^+ and 1 mM paraquat caused a greater than 2-fold increase in 2-OH-E^+; however, this increase was found to be significantly lower than that produced following treatment with menadione. In contrast, MPP^+ and rotenone both elicit a significant increase in ethidium (E^+), E^+-E^+ homodimer, HE-HE homodimer, and HE-E^+ mixed dimer. This indicates an increase in non-specific oxidation of HE (e.g., occurring due to reaction with heme/H_2O_2, perferyl iron, or $^{\bullet}OH$). Previous publications provide evidence for increased $O_2^{\bullet-}$ production following treatment with each of the PD mimetic compounds used here, but have used either electron spin resonance (Klaidman *et al.* 1993), or fluorescence microscopy measurements of HE oxidation (Kalivendi *et al.* 2003). Fluorescence experiments likely detected the large increase in E^+ following treatment with MPP^+ or rotenone, attributing this fluorescence to $O_2^{\bullet-}$. As demonstrated in **Table 1**, the fluorescence emission characteristics of E^+ and 2-OH-E^+ are extremely similar, and are not likely to be resolved with conventional wide-field microscopy. It is likely that other $O_2^{\bullet-}$-independent HE oxidation pathways are involved in the production of E^+, and these are a topic of active investigation.

Recent publications demonstrate a clear mitochondrial involvement in the pathogenesis of Parkinson's disease (Keeney *et al.* 2009, Trimmer & Bennett 2009, Schapira & Jenner 2011). Because increased ROS is proposed to impact mitochondrial function, we next measured total cellular bioenergetic function in N27 cells exposed to PD neurotoxicants. We chose the dopaminergic N27 cell line in which to perform this analysis, as they express tyrosine hydroxylase and the dopamine transporter, but are not differentiated (Adams *et al.* 1996). This is important because many growth factors (e.g., BDNF, α-tocopherol) used to differentiate neuronal cells have known protective effects against the PD mimetic compounds examined here. Furthermore, differentiated neuroblastoma cells (SH-SY5Y cells) have decreased glycolytic function as compared to undifferentiated cells (Schneider *et al.* 2011). Importantly, glycolysis is expected to contribute less to the total ATP production in intact neurons than oxidative phosphorylation because glucose is oxidized completely to CO_2 and H_2O, and ATP production from oxidative phosphorylation is much higher [reviewed in (Clarke & Sokoloff 1999)]. Thus, the non-differentiated N27 cells used here may represent a different metabolic set point than that which is present in the intact brain.

To investigate the relationship between $O_2^{\bullet-}$ production and mitochondrial function, N27 cells were treated with MPP^+ (**Figure 2**), rotenone (**Figure 3**), or paraquat (**Figure 4**). In these experiments, both MPP^+ and rotenone inhibited mitochondrial function as expected, based on previous reports in the literature. Here we show the time-dependence of this inhibition in intact cells for the first time. The effect of paraquat on mitochondrial function is in sharp contrast to the effects of MPP^+ and rotenone. Paraquat, a well-established redox cycling agent, caused a mild, but significant increase in OCR (**Figure 4A**). This most likely represents 1-electron reduction of O_2 to $O_2^{\bullet-}$, as the stimulation is not reversed by addition of mitochondrial inhibitors. Similar observations have been reported using the redox cycling compound 2,3-dimethoxy-1,4-napthoquinone (Dranka *et al.* 2010). Together, these data suggest that the link between superoxide production and mitochondrial dysfunction is not universally correlated in pharmacologic models of Parkinson's disease.

Glycolytic function was also measured in parallel with mitochondrial function following addition of MPP^+ and rotenone. As shown in **Figures 2B** and **3B**, both MPP^+ and rotenone elicited a stimulation in ECAR. This is believed to occur as compensation for inhibition of mitochondrial oxygen consumption – akin to the Warburg effect described in cancer cells (Wu *et al.* 2007, Vander Heiden *et al.* 2009). Stated otherwise: as OCR decreases, ECAR

increases. In both cases, the net effect is a shift from oxidative phosphorylation towards glycolytic metabolism, as indicated in **Figures 2C** and **3C**. In these figures, OCR and ECAR are plotted against each other as a function of the time of the assay. In this way, the shift towards glycolytic metabolism can be seen as an increase in ECAR with the concomitant decrease in OCR – a shift towards the bottom right quadrant of each graph. MPP^+ and rotenone also differ in terms of reversibility of inhibition (**Figure 6**). This reversibility indicates that the underlying mechanism of mitochondrial inhibition differs between these compounds. Notably, this difference in reversibility occurs despite similar levels of $O_2^{\bullet-}$ production (**Figure 1**).

Specific parameters of mitochondrial function were next analyzed according to a previously established protocol using specific mitochondrial inhibitors (**Figure 5**) (Jekabsons & Nicholls 2004, Dranka *et al.* 2011). In addition to MPP^+ and rotenone, we assessed the effects of the toxic metabolite of dopamine, 6-OHDA and paraquat. In this series of experiments, cells were treated with the indicated concentrations of MPP^+, rotenone, 6-OHDA, or paraquat for 4 h, the media was removed, and after washout of the compounds, mitochondrial function was tested. ATP-Linked OCR decreased in response to MPP^+, rotenone, and 6-OHDA, but not paraquat. In addition, MPP^+, rotenone and 6-OHDA decreased the FCCP-stimulated oxygen consumption, here termed maximal OCR. Notably, both rotenone and 6-OHDA caused a decrease in reserve capacity OCR, defined as the difference between the baseline OCR and the FCCP-stimulated rate. In contrast, MPP^+ inhibited maximal OCR, but not to the same degree as rotenone and 6-OHDA. We tentatively assign this observation to the effect of FCCP on the retention of MPP^+ in the mitochondrial matrix due to its positive charge. One suggested mechanism contributing to inhibition of mitochondrial function by MPP^+ is the partial dissipation of the mitochondrial membrane potential ($\Delta\Psi_m$) (Sayre 1989). This is likely to happen due to the Nernstian uptake of the positively charged MPP^+ into the inwardly negative mitochondrial matrix. Despite the initial dissipation of $\Delta\Psi_m$, the remaining potential would serve to retain MPP^+ in the mitochondrial matrix. Treatment with FCCP would then release this MPP^+, alleviating the inhibition of mitochondrial oxygen consumption. In contrast to these results, treatment with paraquat stimulated the baseline OCR, which we found to be due to increased non-mitochondrial OCR (**Figure 5D**).

The stimulation of glycolysis which occurs after treatment with MPP^+ or rotenone is thought to compensate for the decreased mitochondrial oxygen consumption that occurs concomitantly. If true, ATP levels should be maintained. In fact, MPP^+ alone has little effect on ATP levels (**Figure 7**). However, the addition of 2-DG to inhibit glycolysis causes a 50% decrease in ATP levels, which is then exacerbated in the presence of MPP^+. Combined with the lack of ATP depletion in the presence of the ATP-synthase inhibitor oligomycin, these data indicate that N27 cells are typically reliant on glycolysis for ATP production. This finding fits well with previous reports suggesting a protective effect of glucose against MPP^+ toxicity (Mazzio *et al.* 2004). However, here we show for the first time that the compensation of glycolysis for inhibition of OCR happens in parallel following MPP^+ treatment.

While it is clear that oxidative stress and mitochondrial dysfunction are both occurring during PD progression, the lack of a mechanistic connection between these events is also increasingly being recognized (Fukui & Moraes 2008, Surmeier *et al.* 2010). Typically, the progression of Parkinson's disease is thought to occur in a linear (or perhaps circular) fashion. In this model, mitochondrial dysfunction would lead to ROS production, or vice versa. We tested this hypothesis using compounds known to either inhibit mitochondrial Complex I (e.g. rotenone), or redox cycle to produce ROS (e.g. paraquat). Our data suggest that there is not a direct correlation between mitochondrial dysfunction and superoxide

generation. Future studies are required to determine the contribution of the myriad cell types implicated in PD progression. It is clear that some ROS production by glial cells is responsible for loss of dopaminergic neurons (Brown 2007). However, inhibition of ROS is also protective in the absence of the glial cells (Anantharam *et al.* 2007). Conversely, it is unclear why ethyl pyruvate, which should both work as an antioxidant and support mitochondrial function, is only protective against MPP^+ if the glial cells are intact (Huh *et al.* 2011). These and other studies highlight the importance of determining the interrelation of mitochondrial dysfunction and ROS in response to PD neurotoxicant compounds.

Supplementary Material

Refer to Web version on PubMed Central for supplementary material.

Acknowledgments

The authors would like to acknowledge funding from NIH/NINDS grants NS039958 (to B.K.) and NS074443 (to A.K.), and from the Henry R. and Angeline E. Quadracci Chair Endowment (B.K.), and the Eugene and Linda Lloyd Chair Endowment (A.K.). The authors declare that they have no financial conflicts to disclose.

Abbreviations Used

2-OH-E^+	2-Hydroxyethidium
6-OHDA	6-Hydroxydopamine
DPBS	Dulbecco's Phosphate Buffered Saline
ETC	Electron Transport Chain
E^+	Ethidium
ECAR	Extracellular Acidification Rate
FCCP	Carbonyl cyanide-p-trifluoromethoxyphenylhydrazone
HE	Hydroethidine
OCR	Oxygen Consumption Rate
PBS	Phosphate Buffered Saline
PD	Parkinson's disease
RNS	Reactive Nitrogen Species
ROS	Reactive Oxygen Species

References

Adams FS, La Rosa FG, Kumar S, Edwards-Prasad J, Kentroti S, Vernadakis A, Freed CR, Prasad KN. Characterization and transplantation of two neuronal cell lines with dopaminergic properties. Neurochem Res. 1996; 21:619–627. [PubMed: 8726972]

Adams JD Jr. Chang ML, Klaidman L. Parkinson's disease--redox mechanisms. Curr Med Chem. 2001; 8:809–814. [PubMed: 11375751]

Anantharam V, Kaul S, Song C, Kanthasamy A, Kanthasamy AG. Pharmacological inhibition of neuronal NADPH oxidase protects against 1-methyl-4-phenylpyridinium (MPP+)-induced oxidative stress and apoptosis in mesencephalic dopaminergic neuronal cells. Neurotoxicology. 2007; 28:988–997. [PubMed: 17904225]

Beal MF. Bioenergetic approaches for neuroprotection in Parkinson's disease. Ann Neurol. 2003; 53(Suppl 3):S39–47. discussion S47-38. [PubMed: 12666097]

Brown GC. Mechanisms of inflammatory neurodegeneration: iNOS and NADPH oxidase. Biochemical Society Transactions. 2007; 035:1119–1121. [PubMed: 17956292]

Cannon JR, Tapias V, Na HM, Honick AS, Drolet RE, Greenamyre JT. A highly reproducible rotenone model of Parkinson's disease. Neurobiol Dis. 2009; 34:279–290. [PubMed: 19385059]

Castello PR, Drechsel DA, Patel M. Mitochondria are a major source of paraquat-induced reactive oxygen species production in the brain. J Biol Chem. 2007; 282:14186–14193. [PubMed: 17389593]

Clarke, DD.; Sokoloff, L. Circulation and Energy Metabolism of the Brain.. In: Siegel, GJ.; Agranoff, BW.; Albers, RW.; Fisher, SK.; Uhler, MD., editors. Basic Neurochemistry - Molecular, Cellular, and Medical Aspects. Lippincott-Raven; Philadelphia: 1999. p. 638-669.

Collier TJ, Steece-Collier K, McGuire S, Sortwell CE. Cellular models to study dopaminergic injury responses. Ann N Y Acad Sci. 2003; 991:140–151. [PubMed: 12846983]

Czerniczyniec A, Karadayian AG, Bustamante J, Cutrera RA, Lores-Arnaiz S. Paraquat induces behavioral changes and cortical and striatal mitochondrial dysfunction. Free Radic Biol Med. 2011; 51:1428–1436. [PubMed: 21802509]

Davey GP, Peuchen S, Clark JB. Energy thresholds in brain mitochondria. Potential involvement in neurodegeneration. J Biol Chem. 1998; 273:12753–12757. [PubMed: 9582300]

Dorsey ER, Constantinescu R, Thompson JP, et al. Projected number of people with Parkinson disease in the most populous nations, 2005 through 2030. Neurology. 2007; 68:384–386. [PubMed: 17082464]

Dranka BP, Benavides GA, Diers AR, et al. Assessing bioenergetic function in response to oxidative stress by metabolic profiling. Free Radic Biol Med. 2011; 51:1621–1635. [PubMed: 21872656]

Dranka BP, Hill BG, Darley-Usmar VM. Mitochondrial reserve capacity in endothelial cells: The impact of nitric oxide and reactive oxygen species. Free Radic Biol Med. 2010; 48:905–914. [PubMed: 20093177]

Drechsel DA, Patel M. Differential contribution of the mitochondrial respiratory chain complexes to reactive oxygen species production by redox cycling agents implicated in parkinsonism. Toxicol Sci. 2009; 112:427–434. [PubMed: 19767442]

Dunnett SB, Lelos M. Behavioral analysis of motor and non-motor symptoms in rodent models of Parkinson's disease. Prog Brain Res. 2010; 184:35–51. [PubMed: 20887869]

Duty S, Jenner P. Animal models of Parkinson's disease: a source of novel treatments and clues to the cause of the disease. Br J Pharmacol. 2011; 164:1357–1391. [PubMed: 21486284]

Frank DM, Arora PK, Blumer JL, Sayre LM. Model study on the bioreduction of paraquat, MPP+, and analogs. Evidence against a “redox cycling” mechanism in MPTP neurotoxicity. Biochem Biophys Res Commun. 1987; 147:1095–1104. [PubMed: 3499150]

Fukui H, Moraes CT. The mitochondrial impairment, oxidative stress and neurodegeneration connection: reality or just an attractive hypothesis? Trends Neurosci. 2008; 31:251–256. [PubMed: 18403030]

Fukushima T, Yamada K, Isobe A, Shiwaku K, Yamane Y. Mechanism of cytotoxicity of paraquat. I. NADH oxidation and paraquat radical formation via complex I. Exp Toxicol Pathol. 1993; 45:345–349. [PubMed: 8312721]

Gee P, Davison AJ. Intermediates in the aerobic autoxidation of 6-hydroxydopamine: relative importance under different reaction conditions. Free Radic Biol Med. 1989; 6:271–284. [PubMed: 2545550]

Gerencser AA, Neilson A, Choi SW, Edman U, Yadava N, Oh RJ, Ferrick DA, Nicholls DG, Brand MD. Quantitative microplate-based respirometry with correction for oxygen diffusion. Anal Chem. 2009; 81:6868–6878. [PubMed: 19555051]

Ghosh A, Chandran K, Kalivendi SV, Joseph J, Antholine WE, Hillard CJ, Kanthasamy A, Kalyanaraman B. Neuroprotection by a mitochondria-targeted drug in a Parkinson's disease model. Free Radic Biol Med. 2010; 49:1674–1684. [PubMed: 20828611]

Hill BG, Dranka BP, Zou L, Chatham JC, Darley-Usmar VM. Importance of the bioenergetic reserve capacity in response to cardiomyocyte stress induced by 4-hydroxynonenal. Biochem J. 2009; 424:99–107. [PubMed: 19740075]

Huh SH, Chung YC, Piao Y, et al. Ethyl pyruvate rescues nigrostriatal dopaminergic neurons by regulating glial activation in a mouse model of Parkinson's disease. J Immunol. 2011; 187:960–969. [PubMed: 21685323]

Jekabsons MB, Nicholls DG. In situ respiration and bioenergetic status of mitochondria in primary cerebellar granule neuronal cultures exposed continuously to glutamate. J Biol Chem. 2004; 279:32989–33000. [PubMed: 15166243]

Jenner P. Preventing and controlling dyskinesia in Parkinson's disease--a view of current knowledge and future opportunities. Mov Disord. 2008; 23(Suppl 3):S585–598. [PubMed: 18781676]

Jin H, Kanthasamy A, Ghosh A, Yang Y, Anantharam V, Kanthasamy AG. alpha-Synuclein negatively regulates protein kinase Cdelta expression to suppress apoptosis in dopaminergic neurons by reducing p300 histone acetyltransferase activity. J Neurosci. 2011; 31:2035–2051. [PubMed: 21307242]

Johannessen JN, Adams JD, Schuller HM, Bacon JP, Markey SP. 1-Methyl-4-phenylpyridine (MPP+) induces oxidative stress in the rodent. Life Sci. 1986; 38:743–749. [PubMed: 3485234]

Kalivendi SV, Kotamraju S, Cunningham S, Shang T, Hillard CJ, Kalyanaraman B. 1-Methyl-4-phenylpyridinium (MPP+)-induced apoptosis and mitochondrial oxidant generation: role of transferrin-receptor-dependent iron and hydrogen peroxide. Biochem J. 2003; 371:151–164. [PubMed: 12523938]

Keeney PM, Dunham LD, Quigley CK, Morton SL, Bergquist KE, Bennett JP Jr. Cybrid models of Parkinson's disease show variable mitochondrial biogenesis and genotype-respiration relationships. Exp Neurol. 2009; 220:374–382. [PubMed: 19815014]

Klaidman LK, Adams JD Jr. Leung AC, Kim SS, Cadenas E. Redox cycling of MPP+: evidence for a new mechanism involving hydride transfer with xanthine oxidase, aldehyde dehydrogenase, and lipoamide dehydrogenase. Free Radic Biol Med. 1993; 15:169–179. [PubMed: 8397142]

Latchoumycandane C, Anantharam V, Jin H, Kanthasamy A. Dopaminergic neurotoxicant 6-OHDA induces oxidative damage through proteolytic activation of PKCdelta in cell culture and animal models of Parkinson's disease. Toxicol Appl Pharmacol. 2011; 256:314–323. [PubMed: 21846476]

Mazzio EA, Reams RR, Soliman KF. The role of oxidative stress, impaired glycolysis and mitochondrial respiratory redox failure in the cytotoxic effects of 6-hydroxydopamine in vitro. Brain Res. 2004; 1004:29–44. [PubMed: 15033417]

Rodriguez-Pallares J, Parga JA, Munoz A, Rey P, Guerra MJ, Labandeira-Garcia JL. Mechanism of 6-hydroxydopamine neurotoxicity: the role of NADPH oxidase and microglial activation in 6-hydroxydopamine-induced degeneration of dopaminergic neurons. J Neurochem. 2007; 103:145–156. [PubMed: 17573824]

Sayre LM. Biochemical mechanism of action of the dopaminergic neurotoxin 1-methyl-4-phenyl-1,2,3,6-tetrahydropyridine (MPTP). Toxicol Lett. 1989; 48:121–149. [PubMed: 2672418]

Schapira AH. Targeting Mitochondria for Neuroprotection in Parkinson's Disease. Antioxid Redox Signal. 2012

Schapira AH, Jenner P. Etiology and pathogenesis of Parkinson's disease. Mov Disord. 2011; 26:1049–1055. [PubMed: 21626550]

Schneider L, Giordano S, Zelickson BR, M SJ, G AB, Ouyang X, Fineberg N, Darley-Usmar VM, Zhang J. Differentiation of SH-SY5Y cells to a neuronal phenotype changes cellular bioenergetics and the response to oxidative stress. Free Radic Biol Med. 2011; 51:2007–2017. [PubMed: 21945098]

Schulz JB, Beal MF. Neuroprotective effects of free radical scavengers and energy repletion in animal models of neurodegenerative disease. Ann N Y Acad Sci. 1995; 765:100–110. discussion 116-108. [PubMed: 7486598]

Scotcher KP, Irwin I, DeLanney LE, Langston JW, Di Monte D. Mechanism of accumulation of the 1-methyl-4-phenylpyridinium species into mouse brain synaptosomes. J Neurochem. 1991; 56:1602–1607. [PubMed: 2013755]

Snow BJ, Rolfe FL, Lockhart MM, Frampton CM, O'Sullivan JD, Fung V, Smith RA, Murphy MP, Taylor KM. A double-blind, placebo-controlled study to assess the mitochondria-targeted

antioxidant MitoQ as a disease-modifying therapy in Parkinson's disease. Mov Disord. 2010; 25:1670–1674. [PubMed: 20568096]

Surmeier DJ, Guzman JN, Sanchez-Padilla J, Goldberg JA. What causes the death of dopaminergic neurons in Parkinson's disease? Prog Brain Res. 2010; 183:59–77. [PubMed: 20696315]

Tanner CM, Kamel F, Ross GW, et al. Rotenone, Paraquat and Parkinson's Disease. Environ Health Perspect. 2011

Trimmer PA, Bennett JP Jr. The cybrid model of sporadic Parkinson's disease. Exp Neurol. 2009; 218:320–325. [PubMed: 19328199]

Vander Heiden MG, Cantley LC, Thompson CB. Understanding the Warburg effect: the metabolic requirements of cell proliferation. Science. 2009; 324:1029–1033. [PubMed: 19460998]

Votyakova TV, Reynolds IJ. DeltaPsi(m)-Dependent and -independent production of reactive oxygen species by rat brain mitochondria. J Neurochem. 2001; 79:266–277. [PubMed: 11677254]

Wu M, Neilson A, Swift AL, et al. Multiparameter metabolic analysis reveals a close link between attenuated mitochondrial bioenergetic function and enhanced glycolysis dependency in human tumor cells. Am J Physiol Cell Physiol. 2007; 292:C125–136. [PubMed: 16971499]

Yacoubian TA, Standaert DG. Targets for neuroprotection in Parkinson's disease. Biochim Biophys Acta. 2009; 1792:676–687. [PubMed: 18930814]

Zhang D, Anantharam V, Kanthasamy A, Kanthasamy AG. Neuroprotective effect of protein kinase C delta inhibitor rottlerin in cell culture and animal models of Parkinson's disease. J Pharmacol Exp Ther. 2007; 322:913–922. [PubMed: 17565007]

Zhao H, Kalivendi S, Zhang H, Joseph J, Nithipatikom K, Vasquez-Vivar J, Kalyanaraman B. Superoxide reacts with hydroethidine but forms a fluorescent product that is distinctly different from ethidium: potential implications in intracellular fluorescence detection of superoxide. Free Radical Biology and Medicine. 2003; 34:1359–1368. [PubMed: 12757846]

Zielonka J, Hardy M, Kalyanaraman B. HPLC study of oxidation products of hydroethidine in chemical and biological systems: ramifications in superoxide measurements. Free Radic Biol Med. 2009; 46:329–338. [PubMed: 19026738]

Zielonka J, Kalyanaraman B. Hydroethidine- and MitoSOX-derived red fluorescence is not a reliable indicator of intracellular superoxide formation: another inconvenient truth. Free Radic Biol Med. 2010; 48:983–1001. [PubMed: 20116425]

Zielonka J, Zielonka M, Sikora A, Adamus J, Joseph J, Hardy M, Ouari O, Dranka BP, Kalyanaraman B. Global Profiling of Reactive Oxygen and Nitrogen Species in Biological Systems: high-throughput real-time analyses. J Biol Chem. 2012; 287:2984–2995. [PubMed: 22139901]

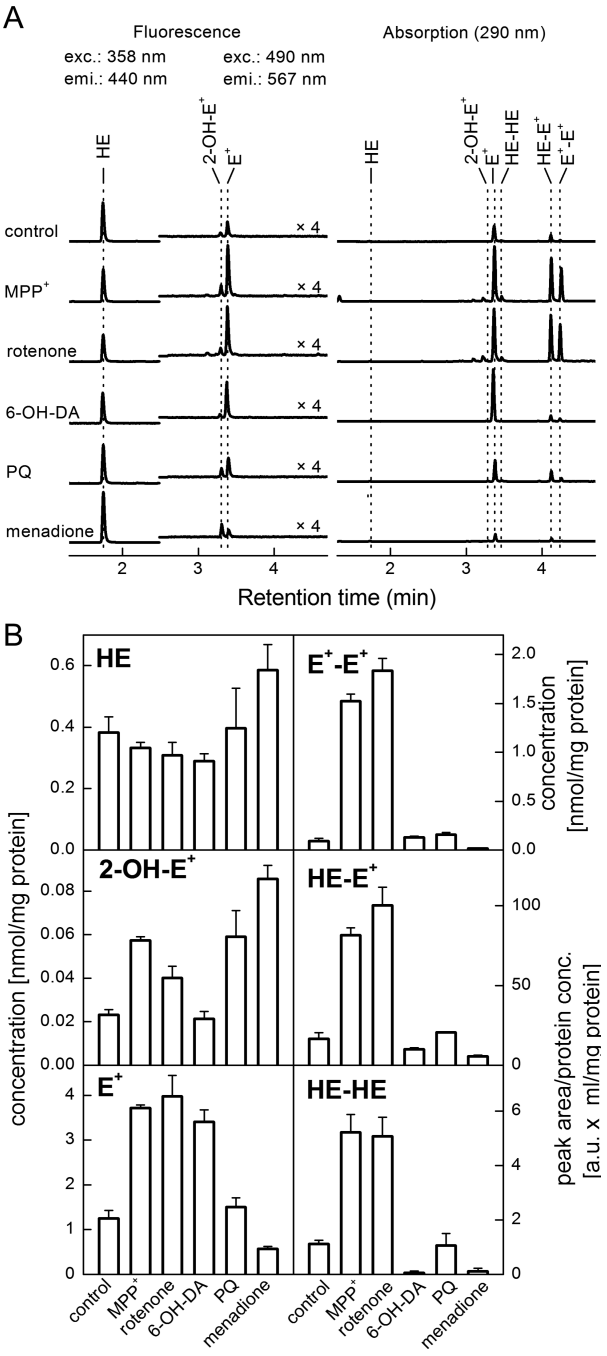

Figure 1. Superoxide production is relatively low following MPP^+, rotenone, or 6-OHDA treatment

N27 cells were grown in 100 mm dishes to 80% confluence. Cells were then treated with MPP^+ (150 μM), rotenone (1 μM), 6-OHDA (100 μM), paraquat (1 mM) or menadione (20 μM) for 4 h. Hydroethidine was added to a final concentration of 10 μM for the final hour of treatment. Cells were washed, and HE oxidation was monitored by HPLC. Panel A: Representative HPLC traces of the oxidation products of HE. Peaks detected by the fluorescence detector are represented on the left, and those detected by absorbance on the right. Panel B: Peak area was quantified and the concentration of HE, 2-OH-E^+, E^+, and E^+-E^+ were determined based on known standards. HE-E^+, and HE-HE amounts are expressed

as measured peak area per mg protein. Data shown are the mean ± sd. n=3 per treatment group.

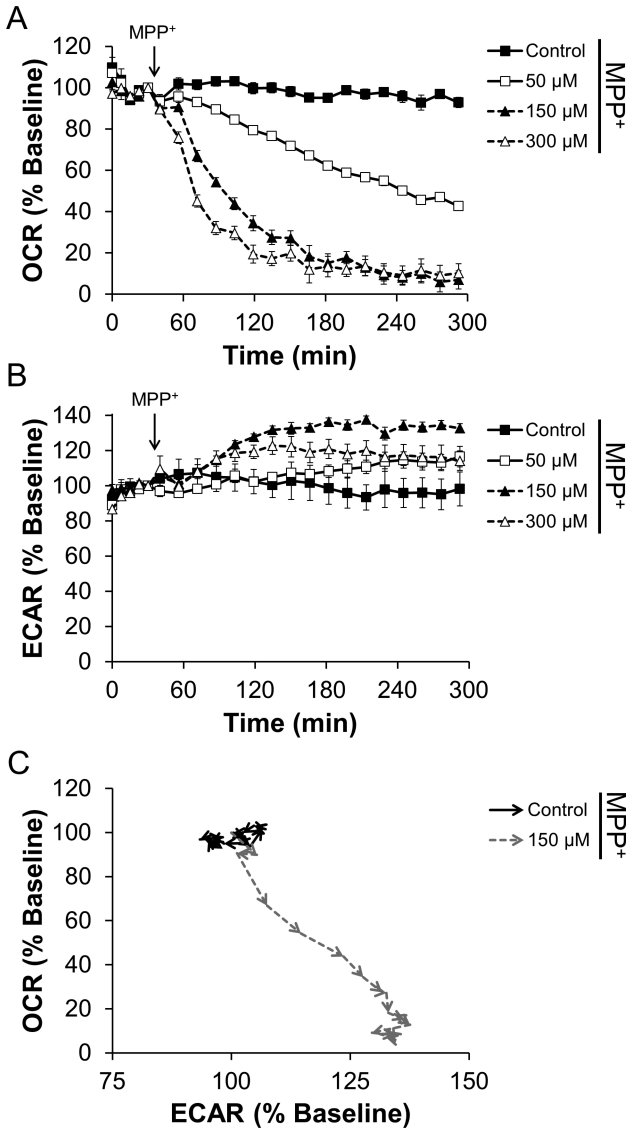

Figure 2. MPP$^+$ inhibits mitochondrial function and stimulates a shift towards glycolytic metabolism

N27 cells were seeded to 4×10^4 cells/well in Seahorse Bioscience V7 tissue culture plates. After 24 h, cells were changed to assay media. Five baseline measurements of OCR and ECAR were recorded and then MPP$^+$ was injected to the final concentrations indicated. Effects on OCR (Panel A) and ECAR (Panel B) were monitored for 4 h. Data in Panels A and B for control and cells treated with 150 μM MPP$^+$ were used to generate the graph in Panel C. OCR and ECAR are plotted against each other for the duration of the experiment. Arrowheads indicate the progression in time, with each arrow point representing a specific data point. Increased ECAR and decreased OCR indicates a shift from oxidative phosphorylation to glycolytic metabolism. For clarity, the first 4 baseline measurements and statistical significance is omitted from data in Panel C. Data shown are the mean ± sem. n=5 per treatment group.

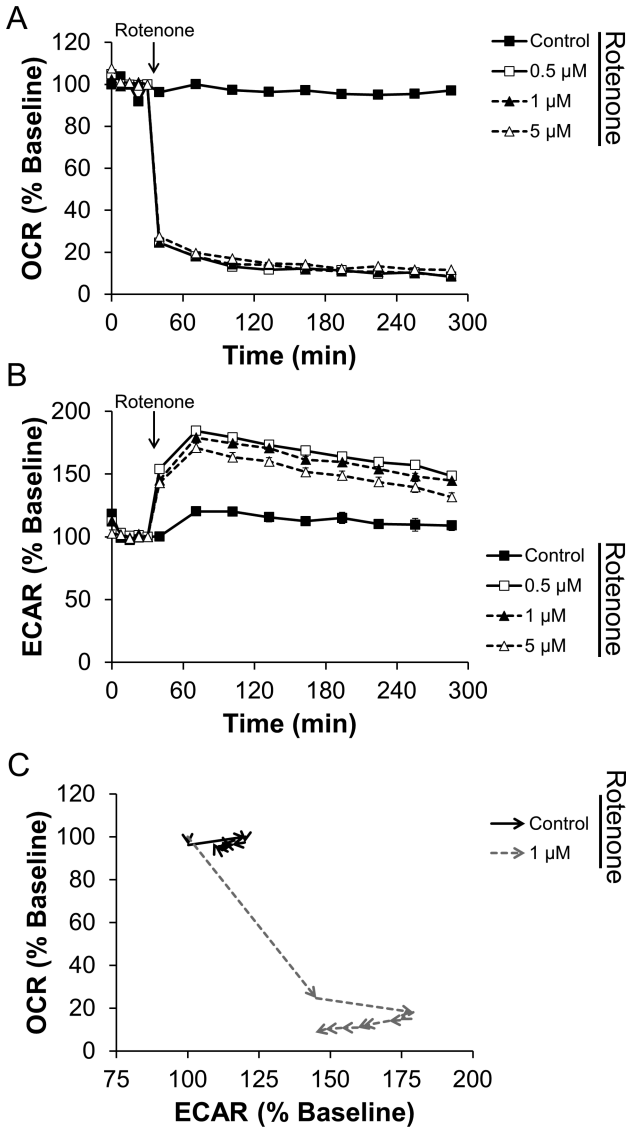

Figure 3. Rotenone rapidly induces a shift towards glycolytic metabolism

N27 cells were seeded and treated as described in Figure 2. The indicated concentration of rotenone was injected after 5 baseline OCR and ECAR measurements, and OCR (Panel A) and ECAR (Panel B) were monitored for an additional 4 h. As in Figure 1, data in Panel C are taken from the cells treated with 1 μM rotenone or left untreated. Arrowheads indicate the progression in time. For clarity, the first 4 baseline measurements and statistical significance is omitted from data in Panel C. Data shown are the mean ± sem. n=5 per treatment group.

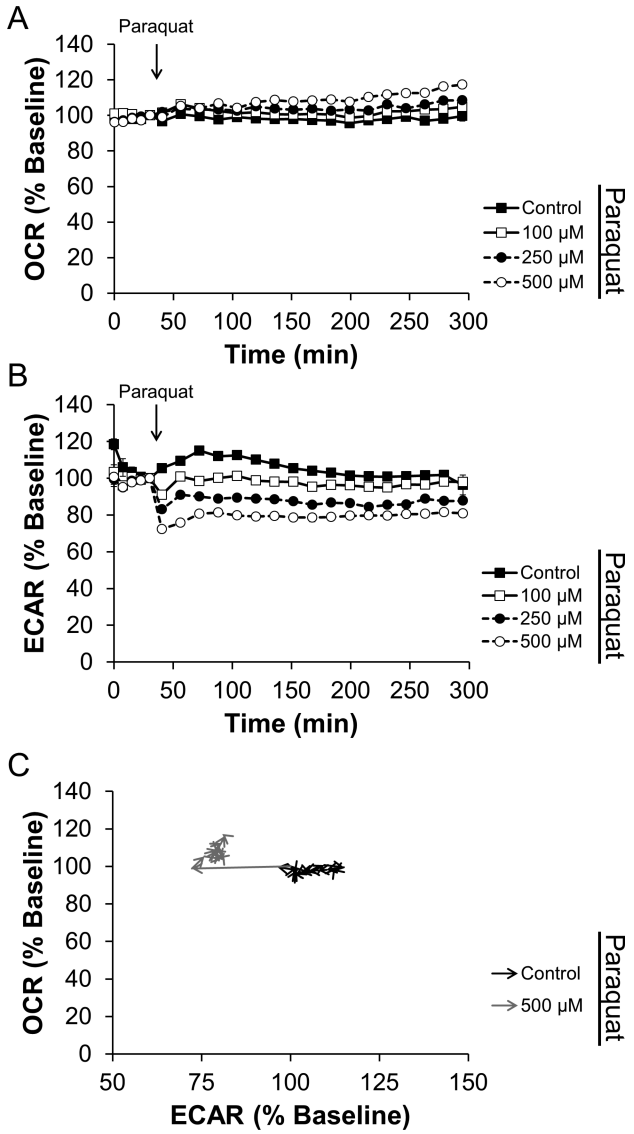

Figure 4. Paraquat has a mild stimulatory effect on oxygen consumption

N27 cells were seeded as described in Figure 2. After baseline OCR and ECAR measurements, paraquat was injected to the final concentrations indicated. OCR (Panel A) and ECAR (Panel B) were monitored for an additional 4 h. As in Figure 2, data in Panel C are taken from the cells treated with 500 μM paraquat or left untreated. Arrowheads indicate the progression in time. For clarity, the first 4 baseline measurements and statistical significance is omitted from data in Panel C. Data shown are the mean ± sem. n=5 per treatment group.

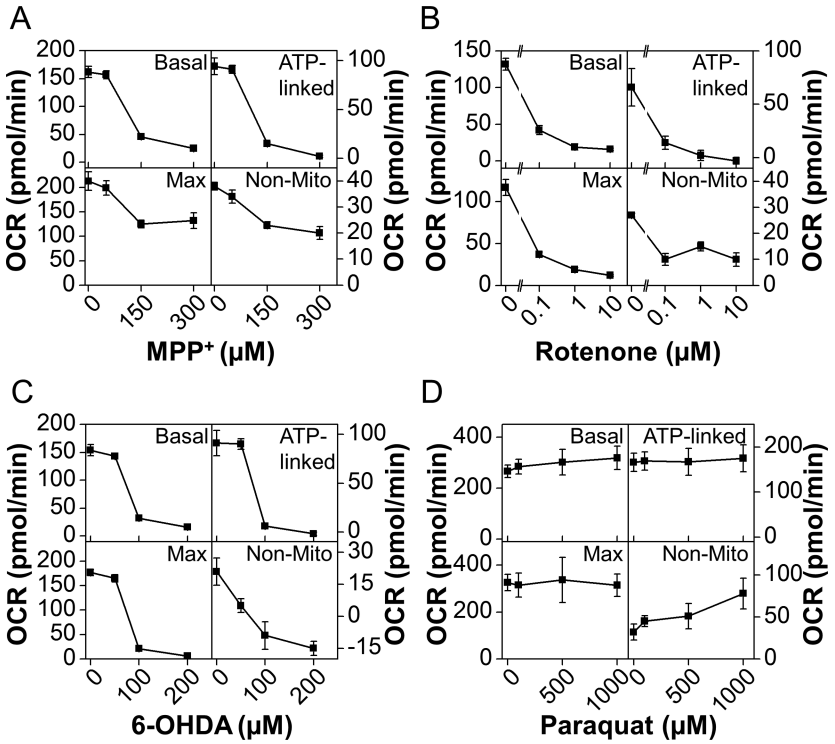

Figure 5. Inhibition of mitochondrial oxygen consumption is at the expense of ATP-linked OCR

N27 cells were seeded to 4×10^4 cells/well in Seahorse Bioscience V7 Tissue Culture plates. After 20 h, cells were treated with MPP^+ (Panel A), rotenone (Panel B), 6-OHDA (Panel C), or paraquat (Panel D) to the final concentrations indicated. The cells were allowed to incubate for 4 h before washing with assay media and analyzing mitochondrial function as described. At least three baseline measurements of OCR were made before injection of oligomycin (1 μg/ml), FCCP (3 μM), and antimycin A (10 μM) in series. Data from these experiments was analyzed as described in the methods to determine the effects on basal OCR, ATP-Linked OCR, Maximal OCR and Non-Mitochondrial OCR (labeled Base, ATP, Max, and Non-Mito respectively). Data shown are the mean ± sem. n=5 per treatment group.

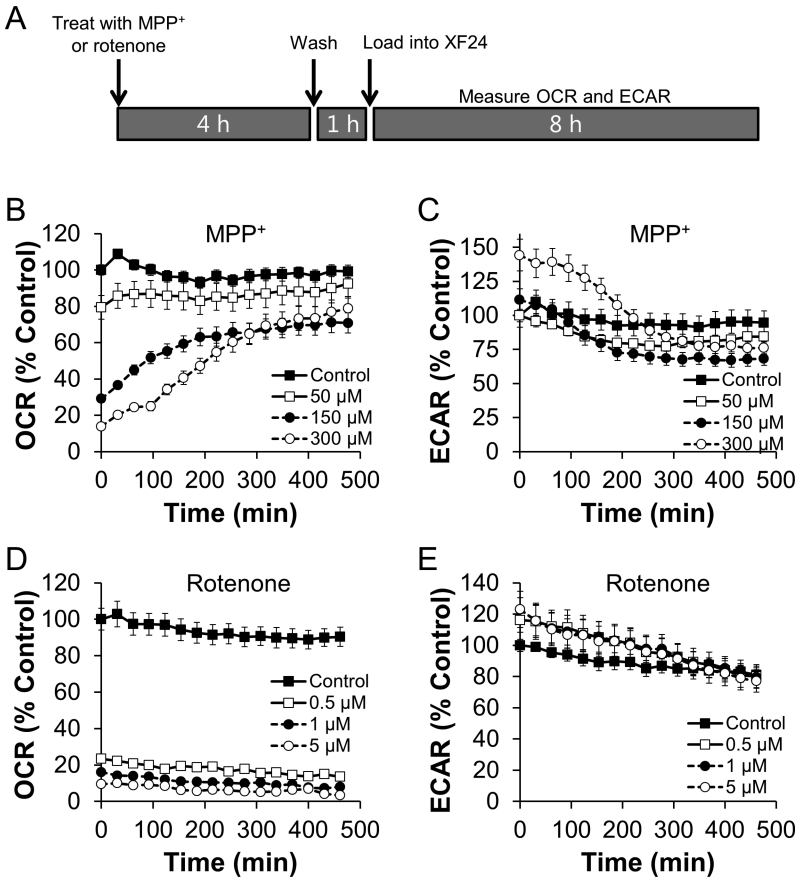

Figure 6. Inhibition of oxygen consumption and stimulation of glycolysis is reversible following MPP^+, but not rotenone treatment

N27 cells were seeded to 4×10^4 cells/well in Seahorse Bioscience V7 Tissue Culture plates. After 20 h, cells were treated with MPP^+ (Panels B and C) or rotenone (Panels D and E) to the final concentrations indicated. The cells were then washed twice with assay media and allowed to incubate in a non-CO_2 incubator for 1 h. The cells were then loaded into the XF24 Analyzer and OCR and ECAR were monitored for 8 h (Shown schematically in Panel A). Data were normalized to the average untreated control value at t=0 for each parameter measured. Data shown are the mean ± sem. n=5 per treatment group. For data in Panels B and C, every other data point was omitted from the graph to increase clarity.

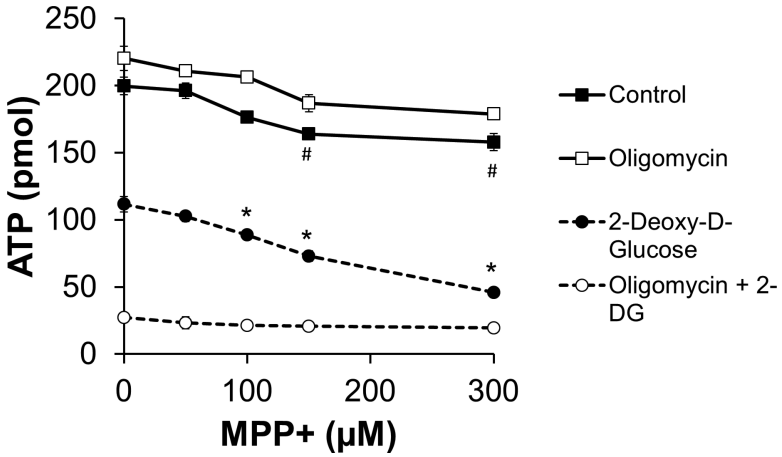

Figure 7. MPP$^+$ decreases ATP levels

N27 cells were seeded to 4×10^4 cells/well in 96 well microplates. After 20 h, cells were cotreated with oligomycin (1 μg/ml), 2-DG (10 mM), or both of these compounds along with the indicated concentration of MPP$^+$. After 4 h, cells were washed and ATP was quantified as described in the methods. Data shown are the mean ± sem. n=4 per treatment group. *, $p\leq0.05$ as compared to 2-DG alone. #, $p\leq0.05$ as compared to PBS-only treated cells. Significance was determined using 2-tailed unpaired t-test.

Table 1

Fluorescence properties of Hydroethidine and its oxidation products.

Probe or Product	Fluorescence excitation λ_{max}	Fluorescence emission λ_{max}
HE	265,348	400
2-OH-E^+	369,470	581
E^+	487	601